# Feature Extraction Method using HoG with LTP for Content-Based Medical Image Retrieval

Original Scientific Paper

**NV Shamna**
P A College of Engineering,
Department of Computer Science and Engineering,
Mangalore, India
shamnanv@gmail.com

**B. Aziz Musthafa**
Beary's Institute of Technology,
Department of Computer Science and Engineering,
Mangalore, India
bazizmusthafa@gmail.com

***Abstract*** *– An accurate diagnosis is significant for the treatment of any disease in its early stage. Content-Based Medical Image Retrieval (CBMIR) is used to find similar medical images in a huge database to help radiologists in diagnosis. The main difficulty in CBMIR is semantic gaps between the lower-level visual details, captured by computer-aided tools and higher-level semantic details captured by humans. Many existing methods such as Manhattan Distance, Triplet Deep Hashing, and Transfer Learning techniques for CBMIR were developed but showed lower efficiency and the computational cost was high. To solve such issues, a new feature extraction approach is proposed using Histogram of Gradient (HoG) with Local Ternary Pattern (LTP) to automatically retrieve medical images from the Contrast-Enhanced Magnetic Resonance Imaging (CE-MRI) database. Adam optimization algorithm is utilized to select features and the Euclidean measure calculates the similarity for query images. From the experimental analysis, it is clearly showing that the proposed HoG-LTP method achieves higher accuracy of 98.8%, a sensitivity of 98.5%, and a specificity of 99.416%, which is better when compared to the existing Random Forest (RF) method which displayed an accuracy, sensitivity, and specificity of 81.1%, 81.7% and 90.5% respectively.*

***Keywords****: CE-MRI dataset, Content-Based Medical Image Retrieval, Histogram of Gradient, Local Ternary Pattern*

## 1. INTRODUCTION

In recent days, computer-aided techniques and tools are frequently employed in medical diagnosis for better health management. Modern computer-aided medical technologies help clinicians in several areas, such as in the diagnosis and treatment of specific diseases [1]. Several computer-based approaches like Computed Tomography, Optical Projection Tomography (OPT), Magnetic Resonance Imaging (MRI), X-Ray, Angiography, Digital Mammography (DM), Ultrasonography, Optical Endoscopy (OE), Nuclear Medical Imaging (NMI), and Positron Emission Tomography (PET), give visual information that aids in the process of medical treatment and diagnosis [2]. This kind of medical photography / imagery offers details about various bodily sections needed for disease detection, diagnosis, monitoring, and therapy [3]. It takes a lot of work to compile computer-aided photographs in one place. Image retrieval has become essential for academicians, companies, and medical institutions to recover crucial information from the database [4]. Content-Based Image Retrieval (CBIR) is used in many industries, including healthcare, law enforcement, criminal justice, and heritage. CBIR is a unique tool for searching visual content amid a bigger amount of data and for retrieving images [5].

Content-Based Medical Image Retrieval (CBMIR) gives suitable results in extracting features from medical data [6]. The content-based retrieval system analyses a particular database consisting of medical images, because the database includes information related to the ranks and features of images. Those that are most comparable to the query photographs are found during retrieval, using similarity characteristics of the database [7]. The present content-based retrieval method retrieves images using similarity measures, lower-level features, and semantic gap reduction [8]. The primary challenge in CBMIR image search is identifying pertinent data amongst available photos for the given que-

ry images. Identification of similar instances based on comparable anatomy acts as a virtual peer review for diagnosis in the field of medicine [9]. Two main issues with the current CBMIR approaches are feature extraction and distance measuring. To increase the efficacy of CBMIR technique, numerous research studies are developed. However, technologies that are now in use are still unable to deliver adequate, and crucial data from image visuals, during the process of medical image retrieval [10]. The major contributions of this research are mentioned as follows,

- A feature extraction method is suggested by combining Histogram of Gradient (HoG) with Local Ternary Pattern (LTP) to automatically obtain medical images from the CE-MRI database in order to boost efficiency and reduce computational cost.
- After that, the Euclidean measure is used to calculate the similarity of the query images, and Adam optimizer is used to choose the features.
- The use of HoG and LTP to automatically retrieve medical images from CE-MRI database is offered as a solution of the Adam Optimizer method for the existing issues.

The remaining paper is given as follows: a review of existing approaches is explained in section 2, and the proposed HoG-LTP used to automatically retrieve medical images from a larger database, is explained in section 3. The results and discussions of the research work are given in section 4. The conclusion along with a brief mention of future work is presented in section 5.

## 2. LITERATURE REVIEW

Techniques based on content-based retrieval of images, that are currently in existence are reviewed in this section. The advantages and limitations of these methods are also described here.

Swati et al. [10] developed an automatic CBIR method based on fine-tuning and transfer learning to retrieve brain tumor-related image content. The features were extracted to identify regions with a brain tumor and were calculated using the Closed Form Metric Learning (CFML) and deep CNN VGG1. Transfer learning approach, along with fine-tuning based block-wise approach was used for the detection of tumor. The performance was carried out on CE-MRI datasets which displayed an improved value of the CFML method in comparison to existing methods. Due to time and space constraints, the method focused solely on tumor retrieval from brain MRI images.

Veerashetty et al. [11] developed an efficient Manhattan distance approach for CBMIR, wherein the histogram of gradients approach was executed. The CBMIR method was divided into two stages: extracting features and matching the features. Initially, the filter of the Gaussian model was used to enhance medical images. The established CBMIR method was used to extract preprocessed features of medical images. Euclidian distance measure was used to calculate and match the similarity between training and testing medical images. The developed method had the advantage of performing better in the retrieval of medical images. However, multiple features that were required to achieve accurate results were not extracted.

A CBMIR method known as Manhattan-distance-based Histogram of Oriented Gradients (M-HOG) was given by Ahmed et al. [12], in which the RGB-based images that were collected were first converted into Hue Saturation Value (HSV) colour space. A group of 18 features was extracted using feature colour and texture function of Grey Level Co-occurrence Matrix (GLCM), and comparable scores were computed. According to the ranking system, top photographs were selected from the query search feedback method. While employing similar coefficients, the performance was increased by means of precision and recall parameters. In the case of extracting features, the application of comparable coefficients to each pixel in the image was a time-consuming operation.

Bressan et al. [13] developed an effective diagnosis method for breast cancer detection that depended on medical active learning for a content-based image retrieval process. The proposed effective diagnosis resulted in high performance in inherent constraints and medical contexts. The group of highly informative images included a selection of conditions like uncertainty and diversity. The similarity developed using an appropriate active learning strategy. Results were evaluated in medical-based queries with an improved precision value given by the developed diagnosis method. The process of learning took more computational time in the presented content-based image retrieval process.

Zhang et al. [14] presented a triplet deep hashing approach based on the image retrieval framework's privacy preservation. Triplet deep Convolutional Neural Network (CNN) was introduced to evaluate the hash codes and visual results. The searching process in the image was improved using a suitable hash code based on S-Tree of Hierarchical Hashing S-Tree (H2S-Tree). The process of retrieving images in the cloud became easier by using an efficient structure of index in triplet deep hashing approach, which also provided an effective learning quality of hash code. Efficiency and accuracy were improved using the proposed triplet deep hashing approach, but the 1024 bits longer hash code resulted in a higher cost of storage.

Khatami et al. [15] developed a parallel deep solution method based on CNN to reduce imbalanced datasets. The majority vote with the HOG, Radon features, and Local Binary Pattern (LBP) was used in finding the best match query images. The capability of the parallel deep solution approach was improved in terms of error rate and accuracy using the IRMA dataset. The parallel deep learning approaches gave very satisfactory results in the process of feature extraction in medical fields, as compared to the existing techniques.

But, the unlabeled datasets and noisy data in the proposed deep solution approach led to unsatisfied results.

The feature extraction technique for multiple object recognition utilizing Histogram of Oriented Gradient (HOG) with Local Ternary Pattern (LTP) was shown by Akanksha and Rao [16]. The suggested technique used the Caltech 101 dataset. The proposed HoG and LTP were used to identify important regions from the image during the feature extraction procedure. Additionally, in order to detect many objects, the Deep Convolutional Neural Network (D-CNN) was utilized to fuse the collected features before sending them to the Region-based Convolutional Neural Network (R-CNN). By successfully extracting the orientation features and texture features, the suggested HoG and LTP feature extraction methods had the advantage of increasing the classification accuracy.

## 3. PROPOSED METHODOLOGY

The architecture and description of the proposed HoG with the LTP method is presented in this section. The diagram of the proposed feature extraction method using HoG with LTP, for CBMIR, is given in Fig. 1.

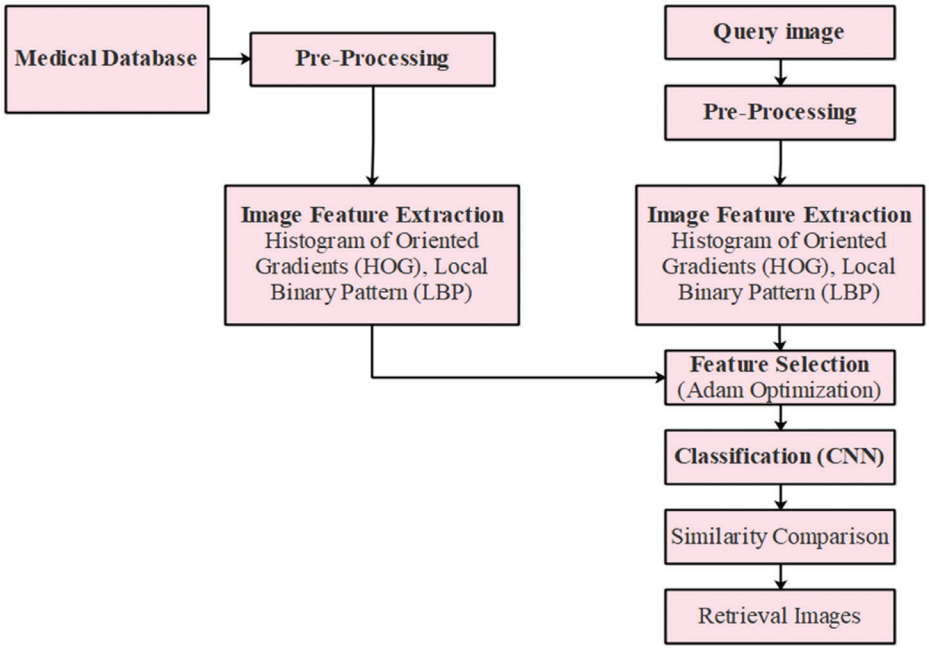


**Fig. 1.** The proposed block diagram of extracting features using HoG with LTP for content-based image retrieval

### 3.1. DATASET AND PREPROCESSING

The publicly accessible Contrast-Enhanced Magnetic Resonance Imaging (CE-MRI) dataset is utilized in the proposed HoG-LTP method. This brain tumor dataset comprises 3064 T1-weighted contrast-enhanced images containing three kinds of brain tumors. It contains 708 slices of images with Meningioma tumor, 1426 slices of tumor images with Glioma, and 930 slices of the tumor with Pituitary, consisting of pixel size

512×512 and the matrix size being 49mm×49mm. The dataset is collected from 233 patients that form a total of 3064 images containing axial, sagittal, and coronal visions. The CE-MRI datasets were gathered from the hospitals of Nan Fang, Guangzhou, China, and the Medical University of Tianjin located in China between 2005 and 2010. The 2D CE-MRI images have high semantic gaps and have tumors of Glioma, Pituitary, and Meningioma. The data is divided into a training set and a test set in the following stages: (i) The proposed system is trained using the training set, which contains 80% of the images, and (ii) The remaining 20% goes to the test set which is classified using the trained network to determine the accuracy.

### 3.2. PREPROCESSING

The collected greyscale images with a pixel size of 512×512 are preprocessed by reframing the size of the images. The size of the image is reduced by resizing it, decreasing the number of pixels by extracting relevant pixels and deleting the unwanted background. The image was framed with new width and height by removing the details of pixels. The same values are proportional to the scale of the image values used for both width and height.

### 3.3. FEATURE EXTRACTION

Grayscale image CE-MRI datasets employ the descriptor without any colour. HOG is used to produce the CE-MRI features, and LBP is used to assess the object's shape and appearance.

#### 3.3.1 Histogram of Gradient

Histogram of Oriented Gradient (HOG) is used to detect the silent parts in the image during feature extraction after the CE-MRI images are preprocessed. The presence of gradient orientation is calculated in the spatial regions of the images, referred to as cells. Gradients of the image are calculated to extract features of HOG and an orientation histogram is created for every cell. Histograms are normalized for every cell, which results in specific blocks of the HOG descriptor. The HOG features are extracted as per the following steps:

The images are converted to greyscale after preprocessing and then are convoluted into vertical and horizontal masks to compute gradients [-1 0 1] and [-1 0 1]^T. Horizontal and vertical mask gradients are represented as shown in equations (1) and (2).

$$G_x(x,y) = [-1\ 0\ 1] * I(x,y) \tag{1}$$

$$G_y(x,y) = [-1\ 0\ 1]^T * I(x,y) \tag{2}$$

Where * represents the convolution; I is the pre-processed image; the orientation at each pixel (θ) that is computed using the gradient ratio in vertical and horizontal directions, is stated as $G_x(x, y)$, $G_y(x, y)$ which is given in equation (3).

$$\theta(x,y) = \arctan\frac{G_x(x,y)}{G_y(x,y)} \tag{3}$$

Further, every block is separated into $M \times N$ cells, where $N \geq M$. Pixels in every image are counted using a weighted vote, which shows the magnitude gradient at every pixel, and the votes are accumulated in orientation bins. The $L$ bins are placed between $0°$ to $180°$ for un-signed gradients or $0°$ to $360°$ for signed gradients, and the $l^{th}$ value of bins is shown in equation (4).

$$\Omega_l(x,y) = \begin{cases} G(x,y) & if\ \theta(x,y) \in bin_l \\ 0 & otherwise \end{cases} \tag{4}$$

Where pixels $(x, y)$ are the magnitude of gradients represented as

$$G(x,y) = \sqrt{G_y(x,y)^2 + G_x(x,y)^2} \tag{5}$$

The features of HOG taken from every cell are stated as $f_{cell}$, and the generated features are the same as the number of bins, wherein the features are represented in equation (6).

$$f_{cell} = \frac{\sum_{(x,y)\in Block} G(x,y)+\epsilon)}{(\sum_{(x,y)\in Block} G(x,y)+\epsilon)} \tag{6}$$

Where $\epsilon$ is an immeasurable smaller quantity, and every cell's normalized features in the block, extracted from dimension vector $d$, are the same as the product of overall cells in the block and oriented bins, which is the final descriptor of the block.

#### 3.2.2. Local Ternary Pattern (LTP)

A three-valued texture operator LTP provides a straightforward and efficient descriptor to describe the features. The new label is extracted from LTP label pixels of the image where the center value of every pixel based on neighborhood threshold is multiplied and added with a power of two. LTP is an extension of LBP where it mostly depends on center pixel values and pixel values existing between threshold (*t*) of *-t* to *+t*, with pixel value as zero. In case the pixel value is greater than the threshold, it results as 1 or -1 of the LTP operator.

The evaluation of the LTP operator is explained in equation (7).

$$LTP(i) = \begin{cases} 1 & if\ t \leq p_i - p_c \\ 0 & if\ |p_i - p_c| < t \\ -1 & if\ -t \geq p_i - p_c \end{cases} \tag{7}$$

Value $t$ represents the user-specified threshold, the pixel value of the neighbor is $p_i$, and $p_c$ is the central value of the pixel. Texture operators are obtained by LTP which are noise sensitive due to not being dependent on center pixel value and grey-level transformations are not followed. The LTP value is classified as upper LTP and lower LTP wherein the upper LTP is developed by applying zeroes for negative values, and lower LTP is obtained by replacing the values of 1 with zeroes and changing the negative values to one in the original LTP. The query images and datasets extract the feature data from HoG and LTP in the feature selection process.

### 3.4. FEATURE SELECTION

The features are selected from the CE-MRI dataset and query images using the Adam optimization algorithm.

#### 3.4.1. Adam Optimization

The traditional stochastic gradient descent is updated as Adam Optimization which is an extension of stochastic gradient descent and productively results in the weights of the updated network. The 1st and 2nd order element is taken in the Adam Optimizer to evaluate the gradient's first-order element (mean of the gradient), and element of second-order (squared gradient based on the element), and then, bias is corrected. The learning rate is divided by the square root of the second-order moment and multiplied by the first-order element to get the update of the final weight.

The three hyper-parameters of LTP are: the learning rate, the decay rate of the first-order moment, and the decay rate of the second-order moment. This work shows that, if the optimal solution is predicted in advance, the learning rate generally takes the final resulting weight, making it simple to estimate the learning rate's scale. Firstly, the exponential moving average is biased towards zero, so it is divided by a number based on the decay rate to get an unbiased value. The Adam optimization algorithm consists of the below steps:

1. The element-wise square and gradient are computed by present parameters.

2. The 1st order and 2nd moment's exponential averages are updated and calculated as unbiased averages.
3. In the Adam optimizer, weight updation is calculated as the average of unbiased 1st order, which is divided by average of the square root of unbiased 2nd order (scaled by a learning rate of 0.001).

According to the Adam optimization algorithm, the weights are computed initially using equation (8).

$$w_t = w_{t-1} - \eta \frac{m_t^1}{\sqrt{v_t}+\epsilon} \quad (8)$$

$$m_t = (1-\beta_1)\sum_{i=0}^{t} \beta_1^{t-i} g_i \quad (9)$$

The second moving momentum is calculated by using equation (10).

$$v_t = (1-\beta_2)\sum_{i=0}^{t} \beta_2^{t-i} g_i^2 \quad (10)$$

The bias correction of momentum is calculated by using equations (11-12).

$$m_t^1 = \frac{m_t}{1-\beta_1^t} \quad (11)$$

$$v_t^1 = \frac{v_t}{1-\beta_2^t} \quad (12)$$

Where, $m_t^{\,1}$ is the moving momentum and $v_t^{\,1}$ is the second moving momentum in Adam optimization.

### 3.1. CLASSIFICATION

The related query images from the end user are extracted by using CNN classifier.

#### 3.5.1 Convolutional Neural Network

The CNN model includes four various layers, presented as follows. The extracted features from input images are fed into convolutional layers, which compute the neurons that are connected to the input of local regions. Each neuron is computed using a dot product of smaller weights and the input image volume is connected. Activation function is then used to determine whether the neurons are right or not. The ReLU layer does not affect the dimensions of the images taken as input. Additionally, the pooling layer reduces the noise effect among the extracted features. Finally, the Fully Connected (FC) layer evaluates the higher-level features. The proposed method uses a pre-trained deep CNN model such as VGG19 to determine the position of the first four lumbar vertebral bodies. The VGG19 network has 19 learnable weight layers, 16 convolutional layers, and 3 FC layers with soft-max. Dropout regularisation is used in the FC layer of VGG19, and ReLU activation function is used in convolutional layers. Convolutional, pooling, ReLU, normalization, and FC layer are all parts of the VGG19 model. The convolutional layer detects the vertebral body by the images as shown in equation (13).

$$g_i^L = b_i^L + \sum_{j=1}^{m_1(L-1)} \psi_{i,j}^L \times h_j^{L-1} \quad (13)$$

Where $g_i^{\,L}$ denotes L output layer, $b_i^{\,L}$ is the base value, $\psi_{i,j}^{\,L}$ is the connection of the filter with $i^{th}$ and $j^{th}$ feature map, and output layer of $L$-1 is $h_j$. The pooling layer detects vertebral foramen in transverse slices and obtains maximum responses from the less convolutional layer to reduce unwanted features and solve the overfitting problem, which is explained using equations (14-16).

$$m_1^L = m_1^{L-1} \quad (14)$$

$$m_2^L = \frac{m_2^{L-1} - F(L)}{S^L} + 1 \quad (15)$$

$$m_3^L = \frac{m_3^{L-1} - F(L)}{S^L} + 1 \quad (16)$$

Where, $S^L$ represents the strides wherein the neural network parameters are changed in the movement of images, $m_1^{\,L}$, $m_2^{\,L}$, and $m_3^{\,L}$ are the feature map filters and the layers; FC and ReLU, are explained in equations (17-18).

$$Re_i^l = max\left(h, h_i^{l-1}\right) \quad (17)$$

$$FC_i^L = f\left(z_i^l\right) with\ z_i^l = \sum_{j=1}^{m_1(l-1)} \sum_{r=1}^{m_2^{l-1}} \sum_{s=1}^{m_3^{l-1}} w_{i,j,r,s}^l \left(FC_i^{l-1}\right)_{r,s} \quad (18)$$

Where the layer of ReLU is represented as $Re_i^l$, $h$ is the output layer, $FC_i^{\,L}$ is the layer of FC that follows the convolutional layer as well as pooling layer, and performs the FC layer activation function for the identification of deeper features.

## 4. RESULTS AND DISCUSSION

### 4.1. SIMILARITY CALCULATION

The Euclidean distance is used to calculate the similarity between CE-MRI images and classified query images. The resemblance between feature dataset and feature vectors of the input query image is calculated. During the image retrieval phase, the global feature vector of the query image is extracted using identified category bank. Finally, similar images from identified semantic category are retrieved and ranked using Euclidean distance between feature vector of the query image and similar candidate images. Effective sequential algorithms generate Euclidean distance maps. The map represents shortest distance from the nearby pixel in the background for each pixel present in the original binary picture's objects. The two picture scans with backward and forward movement of each line, are used to create a map including minor errors. As a result, successful computation is done with parallel propagation, which is an iterative process for expanding/shrinking purpose. In distance mapping, image processing is used frequently. Typically, it is based on one of the metrics calculated using equation (19).

$$d_4\big((i,j),(h,k)\big) = |i-h| + |j-k| \quad (19)$$

which is known as "distance of chessboard," or a combination of it, such as "octagonal distance" in the space of a two-dimensional rectangle with integers *i, j, h,* and *k*.

The binary image includes two sets of pixels labeled 0 and 1, the $L(S)$ which represents the distance map, is an image in which each pixel $(i, j) \in S$ corresponds to a pixel in $L(S)$, wherein the distance map is given in equation (20).

$$L(i,j) = \min\left(d[(i,j),S]\right) \tag{20}$$

Every pixel in $S$ is having a particular $L(S)$ label which is equal to the neighboring distance, hence the same map $L(S)$ is defined for the background.

Content-based medical images are retrieved efficiently using the proposed feature detection; HoG with LTP method, for high-quality data. In contrast to the approaches that existed, this proposed feature detection method gives the desired results in recognizing features using CE-MRI dataset. The retrieval method is applied on a computer with 2.2 GHz, Python 3.7.3 and 8GB RAM. This proposed method demonstrates considerably good performance in extracting features from the image, in comparison to existing algorithms.

### 4.2. PERFORMANCE METRICS

The image retrieval performance of the proposed HoG with LTP uses 70% of training images and 30% of testing images. The proposed HoG with LTP is compared with existing techniques to check the nature of the system parameters. performance metrics considered in the assessment of HoG with LTP are explained as follows:

#### 4.3.1. Accuracy

Accuracy is used to evaluate the model's classification by measuring ratio of the number of right predictions to total number of predictions, which is represented in equation (21).

$$Accuracy = \frac{Number\ of\ correct\ predictions}{overall\ predictions} \tag{21}$$

#### 4.2.2. Sensitivity

Sensitivity measures the ratio of positive values calculated using equation (22).

$$Sensitivity = \frac{TP}{TP+FN} \tag{22}$$

#### 4.2.3. Specificity

Specificity calculates the negative ratio that is predicted correctly and it is calculated using equation (23).

$$Specificity = \frac{TN}{TN+FP} \tag{23}$$

#### 4.2.4. Precision

Precision is the ratio of overall truly classified positives to predicted positives. It is defined in equation (24).

$$Precision = \frac{TP}{TP+FP} \times 100 \tag{24}$$

#### 4.2.5. F-score

F-Score is calculated from the precision and recall of the test model which is expressed in equation (25).

$$F - score = \frac{TP}{TP+1/2(FP+FN)} \tag{25}$$

#### 4.2.6. Error Rate

The measure of error units present in the model is defined as the Error rate and measured by equation (26).

$$Error\ Rate=100\text{-}Accuracy \tag{26}$$

### 4.3. Performance Analysis

The proposed feature detection HoG and LTP methods are used to analyze CE-MRI datasets and provide much more optimal results as compared to existing SVM, RF and RCNN [16]. Results of the proposed HoG and LTP methods are compared to existing models in tables 1 and 2.

**Table1.** Comparison of HoG-LTP method with existing techniques related to sensitivity, specificity, and accuracy for image retrieving

| Methods | Accuracy (%) | Sensitivity (%) | Specificity (%) |
|---|---|---|---|
| **RF** | 81.1 | 81.7 | 90.5 |
| **SVM** | 97.7 | 97.8 | 98.8 |
| **RCNN [16]** | 92.48 | 75.24 | 71.32 |
| **HoG-LTP** | 98.8 | 98.5 | 99.4 |

Table 1 compares the proposed HoG and LTP techniques to the existing techniques which are RF, SVM and RCNN [16]. The proposed method achieves 98.8% accuracy, 98.5% sensitivity, and 99.4% specificity. Whereas the existing RF and SVM respectively obtained an accuracy of 81.1% and 97.7%, sensitivity of 81.7% and 97.8%, and specificity of 90.5% and 98.8%. While the existing RCNN obtains accuracy, sensitivity and specificity at 92.48%, 75.24% and 71.32% respectively. The output of comparison results of the presented HoG with LTP method proves its higher performance when it is compared to previous conventional methods in terms of sensitivity, specificity, and accuracy. Figure 2 compares the proposed HoG with the LTP method to previously existing methods in terms of sensitivity, accuracy, and specificity.

The proposed HoG-LTP method gives higher performance and the error rate is reduced as compared to existing models, which is shown in Figure 3. The retrieved images of Meningioma and Glioma tumors are shown in Fig. 4 and Fig. 5.

**Table 2.** The comparison of HoG-LTP and existing methods in terms of Error rate, Precision, and F-score for images to retrieve features

| Methods | Precision (%) | Error Rate (%) | F-score (%) |
|---|---|---|---|
| **RF** | 90 | 18 | 75 |
| **SVM** | 94 | 2 | 97 |
| **HoG-LTP** | 100 | 1 | 100 |

Table 2 compares the error rate, F-score, and precision of the proposed HoG-LTP method to those of existing techniques such as RF and SVM. The proposed method achieves a precision of 100%, an error rate of 1%, and an F-score of 100%, whereas, for existing models of RF and SVM, the precision value is 90% and 94%, the rate of error is 18% and 2%, and F-Score is 75% and 97%, correspondingly.

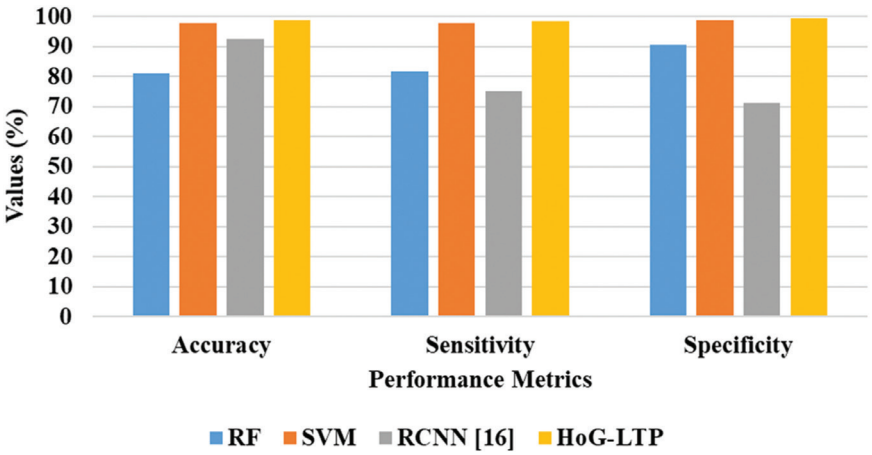


**Fig. 2.** The comparison of HoG-LTP and existing methods in terms of accuracy, sensitivity, and specificity

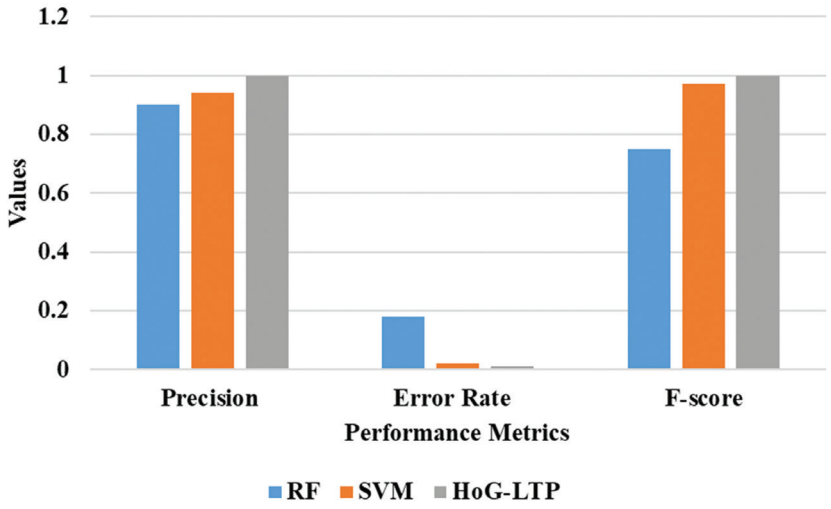


**Fig. 3.** Comparative graph of HoG-LTP with existing methods in terms of error rate, precision, and f-score

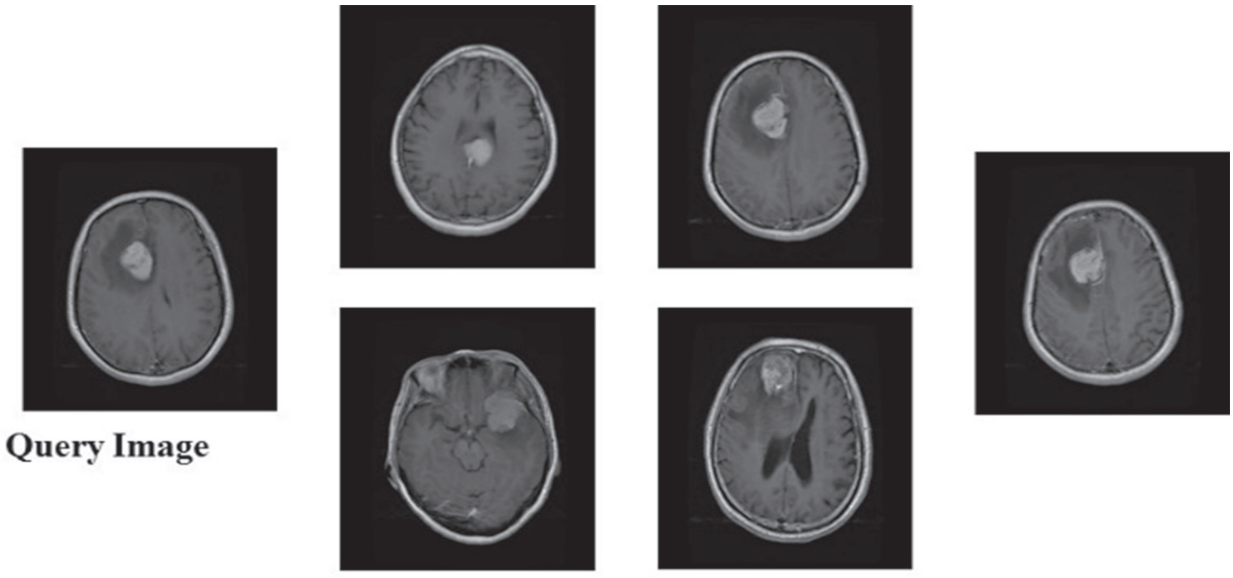


**Fig. 4.** Meningioma tumor query-based retrieved images

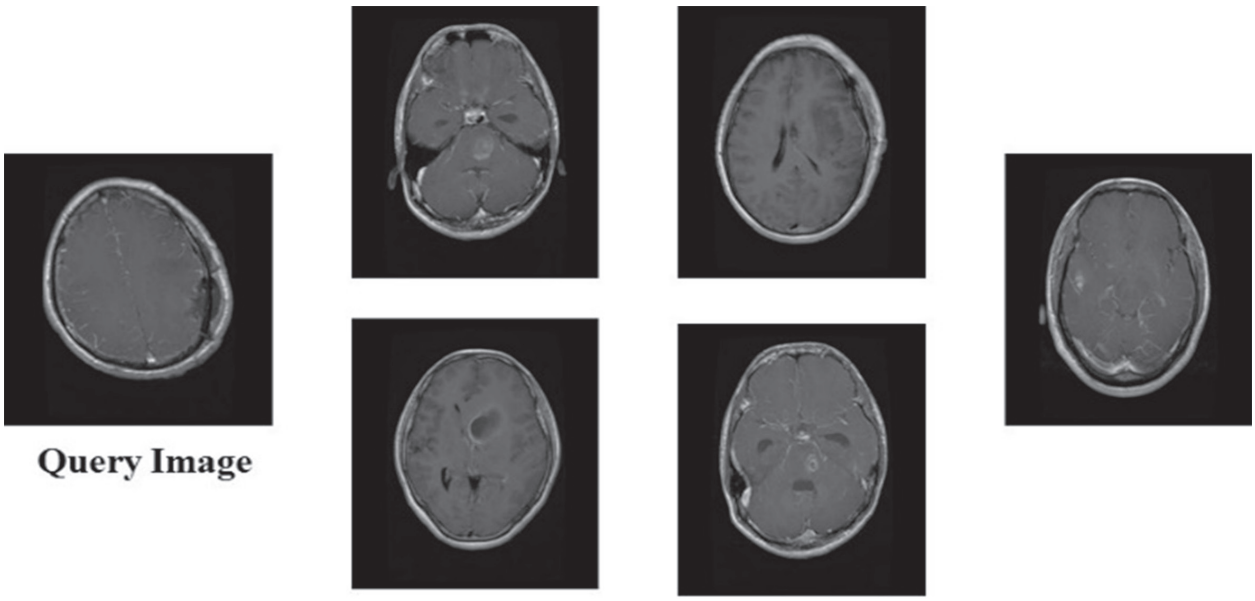


**Fig. 5.** The images that are retrieved for the glioma tumor image query

## 5. CONCLUSION

The main objective of the proposed HoG and LTP models using CB-MIR is, to extract relevant features from medical images for accurate diagnosis of disease. To overcome issues persisting in traditional methods, a novel feature selection method is proposed, which combines HoG and LTP to retrieve medical images automatically from CE-MRI dataset. The size of images in CE-MRI is reconstructed to modify the pixels, which results in a reduction of image size. HOG extracts sufficient information on global features from CE-MRI, and LBP provides an appearance of the object and its shape. Adam optimization algorithm is used to select features from CE-MRI dataset and query images. The extracted features are fed into the CNN classifier, which uses them in the query of images to retrieve from the end-user. Euclidean distance is used to compute the similarity measurement between an input of query image feature vectors and the dataset's feature. Experimental results show that the proposed HoG-LTP technique with CNN classifier, achieves higher performance than existing methods. For future works, various machine learning algorithms will be applied for optimized feature extraction in medical images to reduce the redundant data from the given image datasets.

## 6. REFERENCES

[1] M. Owais, M. Arsalan, J. Choi, K. R. Park, "Effective diagnosis and treatment through content-based medical image retrieval (Cbmir) by using artificial intelligence", Journal of Clinical Medicine, Vol. 8, No. 4, 2019, p. 462.

[2] M. Natarajan, S. Sathiamoorthy, "Heterogeneous Medical Image Retrieval using Multi-Trend Structure Descriptor and Fuzzy SVM Classifier", International Journal of Recent Technology and Engineering, Vol. 8, No. 3, 2019, pp. 3959-3963.

[3] A. Dureja, P. Pahwa, "Medical image retrieval for detecting pneumonia using binary classification with deep convolutional neural networks", Journal of Information and Optimization Sciences, Vol. 41, No. 6, 2020, pp. 1419-1431.

[4] D. B. Renita, C. S. Christopher, "Novel real time content-based medical image retrieval scheme with GWO-SVM", Multimedia Tools and Applications, Vol. 79, No. 23, 2020, pp. 1-17.

[5] M. Garg, G. Dhiman, "A novel content-based image retrieval approach for classification using GLCM features and texture fused LBP variants", Neural Computing and Applications, Vol. 33, No. 4, 2021, pp. 1311-1328.

[6] N. F. Haq, M. Moradi, Z. J. Wang, "A deep community-based approach for large scale content based X-ray image retrieval", Medical Image Analysis, Vol. 68, 2021, p. 101847.

[7] S. Fadaei, A. Rashno, "Content-based Image Retrieval Speedup Based on Optimized Combination of Wavelet and Zernike Features Using Particle Swarm Optimization Algorithm", International Journal of Engineering, Vol. 33, No. 5, 2020, pp. 1000-1009.

[8] M. Kashif, G. Raja, F. Shaukat, "An Efficient Content-Based Image Retrieval System for the Diagnosis of

Lung Diseases", Journal of Digital Imaging, Vol. 33, No. 4, 2020, pp. 971-987.

[9] A. Khatami, M. Babaie, H. R. Tizhoosh, A. Khosravi, T. Nguyen, S. Nahavandi, "A sequential search-space shrinking using CNN transfer learning and a Radon projection pool for medical image retrieval", Expert Systems with Applications, Vol. 100, 2018, pp. 224-233.

[10] L. Tsochatzidis, K. Zagoris, N. Arikidis, A. Karahaliou, L. Costaridou, I. Pratikakis, "Computer-aided diagnosis of mammographic masses based on a supervised content-based image retrieval approach", Pattern Recognition, Vol. 71, 2017, pp. 106-117.

[11] Z. N. K. Swati, Q. Zhao, M. Kabir, F. Ali, Z. Ali, S. Ahmed, J. Lu, "Content-Based Brain Tumor Retrieval for MR Images Using Transfer Learning", IEEE Access, Vol. 7, 2019, pp. 17809-7822.

[12] S. Veerashetty, N. B. Patil, "Manhattan distance-based histogram of oriented gradients for content-based medical image retrieval", International Journal of Computers and Applications, Vol. 43, No. 9, 2021, pp. 924-930.

[13] A. Ahmed, "Implementing Relevance Feedback for Content-Based Medical Image Retrieval", IEEE Access, Vol. 8, 2020, pp. 79969-79976.

[14] R. S. Bressan, P. H. Bugatti, P. T. M. Saito, "Breast cancer diagnosis through active learning in content-based image retrieval", Neurocomputing, Vol. 357, 2019, pp. 1-10.

[15] A. Khatami, M. Babaie, A. Khosravi, H. R. Tizhoosh, S. Nahavandi, "Parallel deep solutions for image retrieval from imbalanced medical imaging archives", Applied Soft Computing, Vol. 63, 2018, pp. 197-205.

[16] E. Akanksha, P. R. K. Rao, "A Feature Extraction Approach for Multi-Object Detection Using HoG and LTP", International Journal of Intelligent Engineering and Systems, Vol. 14, No. 5, 2021, pp. 259-268.